ACS APPLIED MATERIALS & INTERFACES

Research Article

www.acsami.org

Porphyrin Metalation at the MgO Nanocube/Toluene Interface

Johannes Schneider,[†] Fabian Kollhoff,[‡] Johannes Bernardi,[§] Andre Kaftan,[‡] Jörg Libuda,*[,‡,⊥] Thomas Berger,*[,†] Mathias Laurin,[‡] and Oliver Diwald[†]

[†]Department of Materials Science and Physics, Paris Lodron University of Salzburg, Hellbrunnerstrasse 34/III, A-5020 Salzburg, Austria

[‡]Lehrstuhl für Physikalische Chemie II, Friedrich-Alexander-Universität Erlangen-Nürnberg, Egerlandstraße 3, 91058 Erlangen, Germany

[§]University Service Center for Transmission Electron Microscopy, Vienna University of Technology, Wiedner Hauptstrasse 8-10, A-1040 Vienna, Austria

[⊥]Erlangen Catalysis Resource Center and Interdisciplinary Center for Interface-Controlled Processes, Friedrich-Alexander-Universität Erlangen-Nürnberg, 91058 Erlangen, Germany

Supporting Information

ABSTRACT: Molecular insights into porphyrin adsorption on nanostructured metal oxide surfaces and associated ion exchange reactions are key to the development of functional hybrids for energy conversion, sensing, and light emission devices. Here we investigated the adsorption of tetraphenyl-porphyrin (2HTPP) from toluene solution on two types of MgO powder. We compare MgO nanocubes with an average size $d < 10$ nm and MgO cubes with 10 nm $\leq d \leq$ 1000 nm. Using molecular spectroscopy techniques such as UV/vis transmission and diffuse reflectance (DR), photoluminescence (PL), and diffuse reflectance infrared Fourier-transform (DRIFT) spectroscopy in combination with structural characterization techniques (powder X-ray diffraction and transmission electron microscopy, TEM), we identified a new room temperature metalation reaction that converts 2HTPP into magnesium tetraphenyl-porphyrin (MgTPP). Mg^{2+} uptake from the MgO nanocube surfaces and the concomitant protonation of the oxide surface level off at a concentration that corresponds to roughly one monolayer equivalent adsorbed on the MgO nanocubes. Larger MgO cubes, in contrast, show suppressed exchange, and only traces of MgTPP can be detected by photoluminescence.

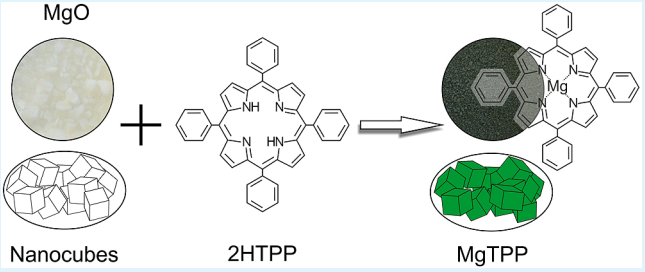

KEYWORDS: *porphyrin metalation, MgO cubes, solid−liquid interface, molecular spectroscopies, dye adsorption, hybrid materials*

INTRODUCTION

The functionalization of nanostructured metal oxides with organic molecules and the implementation of the resulting organic−inorganic hybrids into devices[1,2] require detailed knowledge about the reactivity and stability of the inorganic−organic interfaces in different chemical environments. Current challenges in the functionalization and processing of related materials call for detailed studies of the adsorption and surface reactions at a molecular level. Toward this aim, tailored and well-defined model particle systems with interface properties that are straightforwardly accessible to experiment are indispensable.[3]

Microscopic level insight into the interface between the organic molecule and the oxide material and into interfacial electron and proton transfer processes is particularly important for emerging applications in solar energy conversion, photocatalytic reactors, electrochromic devices, or new materials for sensing and rewritable storage media.[4,5] With regard to the functionalization of metal oxide nanoparticles with organic dyes, there is only little quantitative information available on adsorption strength and adsorbate coverage. As a consequence of the immanent complexity of the material, preconditioning of the metal oxide particle surface and its reactivity require more attention than typically paid to this issue in the past.[6,7]

Another important aspect of nanoparticle functionalization with dyes relates to the metastable nature of nanomaterials. Because their properties are largely determined by the nature and composition of the interface, they are expected to respond to the removal of the surrounding medium.[8]

The functionalization of MgO surfaces with organic molecules is important for a variety of functional materials and resulting applications. In dye-sensitized solar cell research, interlayers of insulating MgO have been reported to significantly improve the performance of solid state and liquid electrolyte-based devices.[9,10] Both electronic (band edge shifts, increase of the electron lifetime) and optical effects (increased

Received: July 9, 2015
Accepted: October 5, 2015
Published: October 5, 2015

DOI: 10.1021/acsami.5b08123
ACS Appl. Mater. Interfaces 2015, 7, 22962−22969

dye loading) have been claimed to contribute to the performance increase. The underlying mechanisms of the beneficial effects, however, are still under debate.[11]

Another important application field of high surface area MgO materials, which still poses considerable challenges for interface science and technology, is the removal of organic dyes from effluents. Recent reports have highlighted the outstanding adsorption properties of mesoporous MgO architectures.[12,13] Although mechanistic details of the reactions that give rise to high adsorption capacity and adsorption rates are not yet fully understood, electrostatic interaction forces and surface complexation are considered to be crucial issues in this context.

The present study aims at the structural characterization of MgO materials before and after functionalization with tetraphenyl-porphyrin (2HTPP). We employ complementary molecular spectroscopic techniques to investigate the activation of porphyrin molecules dissolved in toluene at the toluene−MgO interface. For the functionalization approach we used MgO nanoparticles that were grown in the gas phase and which exhibit bare and dehydroxylated oxide surfaces after further vacuum processing.[14] Because we immersed the nanoparticle powder into toluene solutions of the porphyrin, several aspects of the functionalization process have to be taken into account such as solvent- and porphyrin-induced particle erosion, as well as changes of the particle aggregation. Understanding these effects is essential to discriminate between spectroscopic changes induced by adsorption and surface chemistry, on the one hand, and those that arise from the modification of the microstructure of the particle, which may originate from materials functionalization.[15,16]

We employed powders of vapor phase grown cubic MgO particles.[14] The absence of solvents during particle nucleation and growth prevents substantial particle aggregation and sintering during annealing and provides, in terms of microstructure, a well-defined starting point to study molecular adsorption at the interface between liquids and nanostructured solids. Both model particle systems, MgO *nanocubes* obtained by chemical vapor synthesis (CVS) and larger MgO *cubes*, which were prepared by Mg combustion in air, are well-defined in terms of morphology.[17] We annealed all particle powders in high vacuum as well as in pure oxygen atmosphere to eliminate surface contaminants that may affect the adsorption process. With the present study we demonstrate for the first time a heterogeneous metalation reaction that involves a free base porphyrin as educt species and MgO particles as adsorbent and Mg^{2+} ion source. Supported by results from quantitative adsorption experiments, this study shows that it is feasible to gain a high level of control over adsorption chemistry at organic−inorganic interfaces using an integrated characterization approach.

EXPERIMENTAL SECTION

Material Synthesis and Activation. MgO *nanocube* powders were prepared by CVS.[18] The CVS reactor consists of two concentric quartz glass tubes placed inside a cylindrical furnace. The inner tube hosts ceramic ships containing Mg pieces (99.98%, Alfa Aesar). Heating to 913 K guarantees a metal vapor pressure of 1 mmHg column (1.33 mbar). An argon stream (Ar 5.0) transports the metal vapor from the evaporation zone to the end of the inner glass tube. At this position the argon/metal vapor mixture comes in contact with molecular oxygen from the outer glass tube. The exothermic oxidation reaction gives rise to a bright flame in the reactor, and MgO nanoparticles are formed as a result of homogeneous nucleation in the gas phase. Stable process conditions are guaranteed by the spatial separation of the Mg evaporation and oxidation zone. Furthermore, continuous pumping keeps the residence time of resulting nuclei within the flame short and prevents substantial coarsening and coalescence.

Larger MgO *cubes* were synthesized by combustion of Mg pieces (99.98%, Alfa Aesar) in air. A glass-plate was kept at a constant height (~10 cm) above the combustion zone, allowing for the collection of particles near the generation zone.

After production, the two types of MgO powders—ensembles of MgO *nanocubes* and those of larger sized *cubes*—were transferred into quartz glass cells, which allow thermal activation of the powders in vacuum ($p < 10^{-5}$ mbar) as well as in defined gas atmospheres. Cleaning of the as-obtained MgO powders and removal of organic contaminants is carried out by heating to 1123 K at a rate of 10 K min^{-1} in high vacuum ($p < 10^{-5}$ mbar) and subsequent exposure to molecular oxygen at this temperature. Then, at pressures $p < 5 \times 10^{-6}$ mbar the sample temperature was raised to 1173 K and kept for 1 h at this temperature until full dehydroxylation of the sample surface was achieved.[19] The activated MgO *nanocubes* are characterized by a narrow particle size distribution below 10 nm. The larger MgO *cubes* show a very broad size distribution in the range 10 nm $\leq d \leq$ 1000 nm.[17]

Adsorption Experiments. 2HTPP (98%, Porphyrin Systems) was immersed into anhydrous toluene (99.8%, Sigma-Aldrich) and stirred for 24 h at room temperature upon quantitative dissolution. Afterward, 400 mg of MgO powder was dispersed in 25 mL of the porphyrin solution. Stirring at room temperature for another period of 24 h guarantees that the adsorption equilibrium is established. During this procedure the flask was wrapped in aluminum foil to protect the suspension from daylight and unwanted photochemical reactions. Subsequently, MgO particles were separated from the toluene solution by centrifugation (8 min, 4000 min^{-1}). The supernatant solution was decanted, and the solid fraction was redispersed and washed repeatedly in fresh toluene to efficiently remove weakly bound porphyrin molecules. Five washing cycles were performed, and the composition and the porphyrin concentration of the resulting washing solutions were determined by UV/vis spectroscopy. The solid fraction was dried using a membrane pump and finally transferred into a quartz glass cuvette for further drying at pressures $p < 5 \times 10^{-6}$ mbar using the vacuum of a turbomolecular pump. This cell was used for diffuse reflectance (DR) and photoluminescence (PL) measurements. The amount of adsorbed porphyrin was inferred from the photometrically determined porphyrin concentration inside the supernatant solution. This procedure was carried out before contact of the MgO nanocubes with the porphyrin solution and after the adsorption equilibrium being established.

Material Characterization: Structure, Morphology, and Size Distribution. Before and after porphyrin adsorption, X-ray diffraction (XRD) on the MgO powders was measured on a Bruker AXS D8 Advance diffractometer using Cu Kα radiation (λ = 154 pm). Small amounts of the powders were cast on a carbon grid for investigation with a TECNAI F20 transmission electron microscope equipped with a field emission gun and an S-twin objective lens.

Spectroscopy. A PerkinElmer Lambda 750 spectrometer was used to record UV/vis transmission spectra of porphyrin solutions. UV/vis diffuse reflectance (DR-UV/vis) spectra of MgO powders were acquired using an integrating sphere. After porphyrin adsorption from the liquid toluene phase, the samples were transferred to an optical high-vacuum cell, which allows for powder drying down to pressures of $p < 5 \times 10^{-6}$ mbar. All UV/vis DR spectra were recorded in the presence of 100 mbar of O_2 to quench luminescence, which would interfere with the optical absorption measurements. Photoluminescence emission spectra of the powders, on the other hand, were measured in the same cuvette at $p < 5 \times 10^{-6}$ mbar using an Edinburgh instruments FLS 980 spectrometer.

The IR spectra presented here were performed in diffuse reflectance infrared Fourier-transform (DRIFT) mode using an open sample cup placed in a Praying Mantis DR accessory (Harrick). The IR spectrometer is a Bruker 80/v spectrometer. The sample chamber was evacuated for at least 30 min before the measurements to allow

DOI: 10.1021/acsami.5b08123
ACS Appl. Mater. Interfaces 2015, 7, 22962−22969

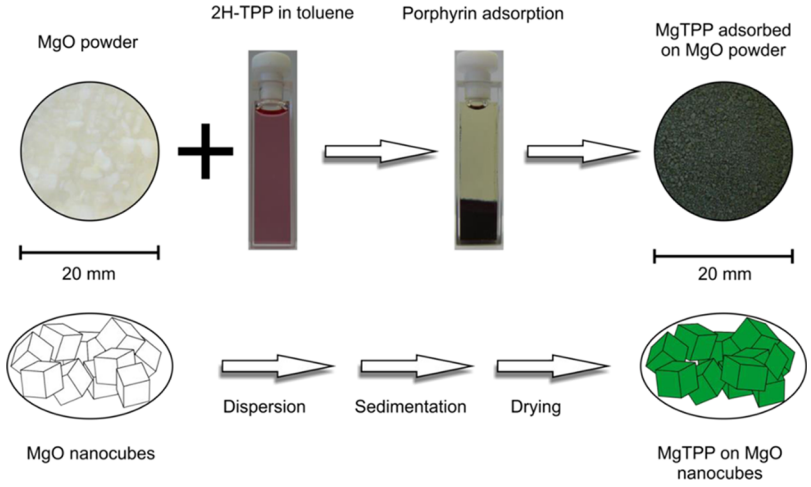

Figure 1. Scheme illustrating the experimental procedure of 2HTPP adsorption at MgO nanocubes, which by porphyrin metalation leads to the discoloration of the porphyrin solution and coloration the MgO nanocube powder. Further details about the different steps of powder treatment are provided in the text.

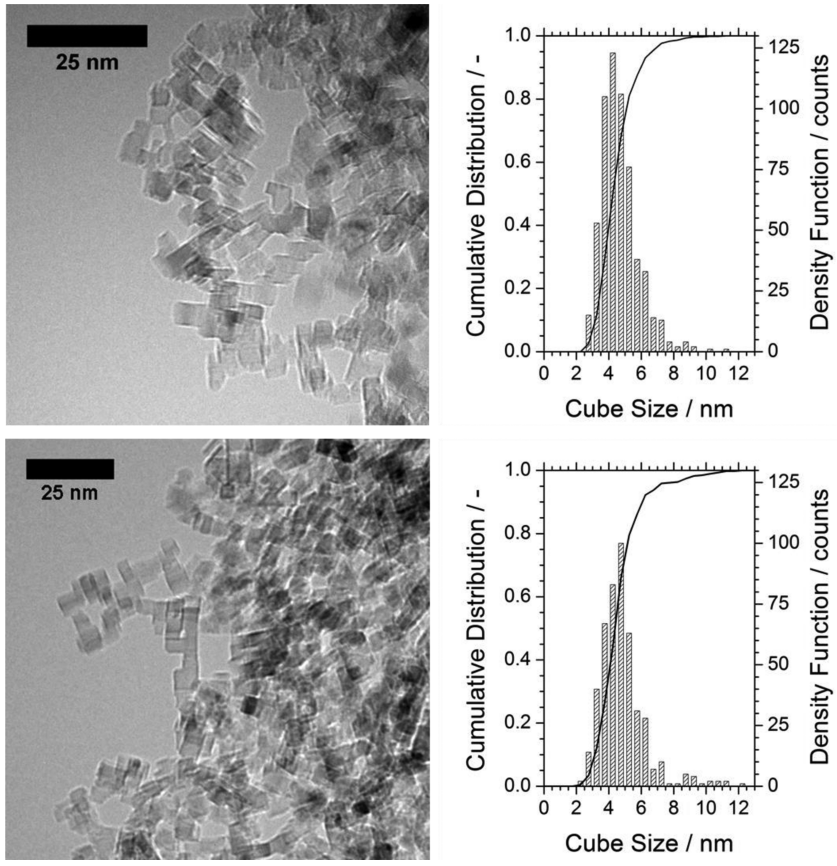

Figure 2. Transmission electron micrographs and particle size distribution plots of MgO nanocubes before (top) and after porphyrin adsorption (bottom). Porphyrin concentration = 6×10^{-3} mol L^{-1}.

pumping of atmospheric water and CO_2. For the background we acquired spectra on nonfunctionalized MgO nanocube and cube powders, respectively.

RESULTS

Contact of a MgO nanocube powder with a 2HTPP solution produces significant optical changes in the supernatant solution as well as in the powder (Figure 1). Starting at low porphyrin concentrations ($c < 1 \times 10^{-3}$ mol L^{-1}), the color of the initially purple solution (left quartz glass cell in Figure 1) fades and we obtain a colorless clear solution (right quartz glass cell in Figure 1). At the same time, the originally white MgO powder adopts a dark green color.

Despite significant changes of the optical properties of the material, there are no structural, microstructural, or morphological changes of the MgO crystallites as evidenced by X-ray diffraction (Figure S1) and transmission electron microscopy (TEM) (Figure 2 and Figure S2). Both the size distributions

DOI: 10.1021/acsami.5b08123
ACS Appl. Mater. Interfaces 2015, 7, 22962−22969

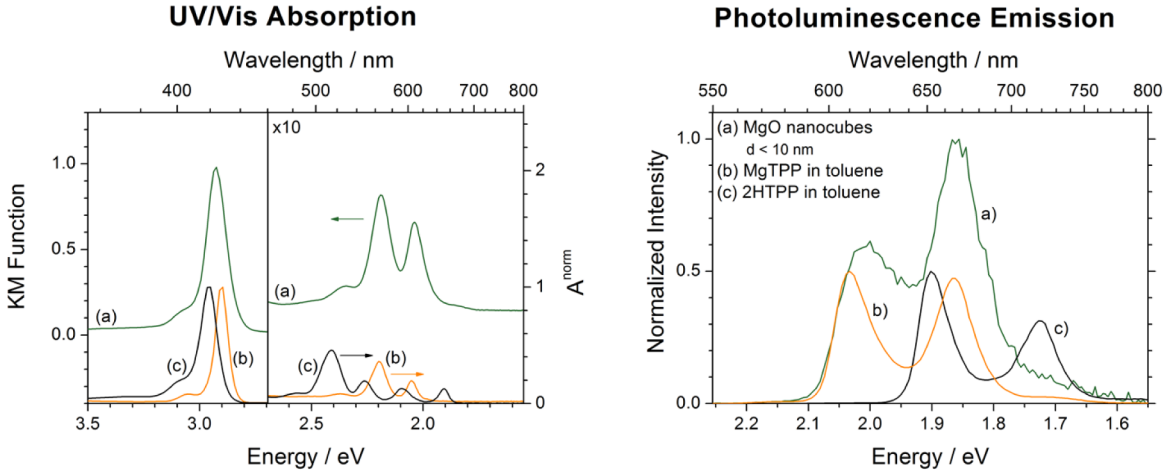

Figure 3. UV/vis DR spectra (left) and photoluminescence emission spectra (right) of MgTPP adsorbed on MgO nanocubes (a) as well as MgTPP and 2HTPP in toluene (b and c, respectively). The porphyrin was adsorbed on MgO nanocubes from an anhydrous toluene solution with a 2HTPP concentration of 10^{-5} mol L^{-1}.

and the shape of the nanocubes are retained after performing the experimental sequence comprising (i) the dispersion of a MgO nanocube powder in a porphyrin toluene solution, (ii) centrifugation and sedimentation, (iii) multiple washing steps with fresh anhydrous toluene solution (five times), and (iv) the removal of the liquid phase and subsequent drying under high-vacuum conditions (Figure 1).

Molecular spectroscopy was used to resolve the molecular origin of the optical changes observed in the material (Figures 1 and 3a, left). The absorption spectrum of porphyrins in the UV/vis range results from two characteristic contributions: an intense absorption band in the range between 3.1 eV > E > 2.5 eV (400 nm < λ < 500 nm, Figure 3b,c, left), which is attributed to the B- (or Soret)-band related to the $S_0 \rightarrow S_2(\pi, \pi^*)$ transition.[20]

In addition, weaker bands in the range 2.5 eV > E > 1.8 eV (500 nm < λ < 700 nm), referred to as Q-bands, are consistent with $S_0 \rightarrow S_1(\pi, \pi^*)$ transitions that are split into different vibrational states (Q(0,0) and Q(0,1)). Whereas the UV/vis spectra of free-base porphyrins show four Q-bands (Figure 3c, left), the higher symmetry of the molecular center in the metalated porphyrin gives rise to a simple spectrum with only two Q-bands (Figure 3b, left).[21,22]

After MgO nanocube dispersion in a 2HTPP solution and subsequent drying, the UV/vis DR spectrum of the MgO *nanocube* powder shows an intense Soret-band at 2.92 eV (425 nm) and two additional well-separated bands at 2.19 eV (565 nm) and 2.03 eV (610 nm) (Figure 3a, left). Furthermore, a low-intensity band is observed at 2.34 eV (530 nm). Comparison of this spectral region with that of 2HTPP and magnesium tetraphenyl-porphyrin (MgTPP) in solution showing the above-mentioned Q-bands (Figure 3b,c, left) provides first evidence for adsorptive metalation of porphyrin at the toluene−MgO interface and at room temperature.

After contact of the MgO *nanocube* powder with the porphyrin solution, the respective PL emission spectrum reveals two bands at 2.00 eV (620 nm) and at 1.85 eV (670 nm) as well as a minor contribution at 1.72 eV (720 nm) (Figure 3a, right). With regard to the energies of the band maxima, the two main emission bands are in good agreement with those measured for the MgTPP in toluene solution (Figure 3b, right). The contribution at 1.72 eV (720 nm) together with the deviation of the relative band intensities at 2.03 eV (610 nm) and at 1.86 eV (665 nm) from those of the MgTPP fingerprints is attributed to minor contributions from free-base porphyrin. Consistent with UV/vis DR, photoluminescence provides further evidence for the metalation of the porphyrin at room temperature on the MgO nanocube surface.

The number of adsorbed and metalated porphyrin molecules per MgO nanocube was photometrically determined using 2HTPP solutions with different initial concentrations (Figure 4). In porphyrin solutions with initial concentrations c < 1 ×

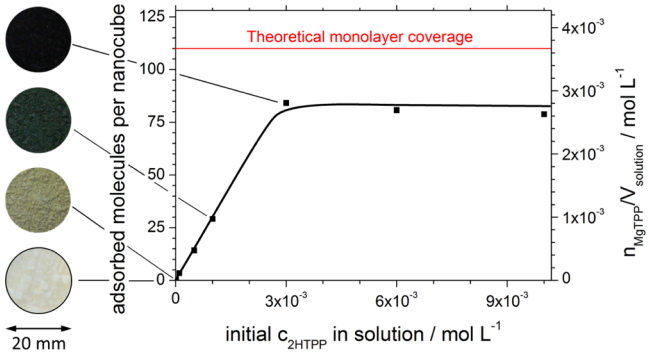

Figure 4. Number of adsorbed MgTPP molecules per nanocube as a function of the initial 2HTPP concentration in toluene solution.

10^{-3} mol L^{-1}, quantitative adsorption and metalation was observed and demonstrated by the complete discoloration of the supernatant solution (right quartz glass cell of Figure 1). At 2HTPP concentrations c > 5 × 10^{-3} mol L^{-1} the number of adsorbed molecules saturates at a level that corresponds to 80 ± 5 molecules per MgO nanocube. Considering a nanocube with an edge length of 6 nm and assuming an area of 2 nm^2 for the spatial requirement of the flat-lying 2HTPP molecule,[23,24] this concentration is of the order of one monolayer equivalent. All powders were washed five times with anhydrous toluene to remove weakly bound molecules. From the UV/vis DR spectrum acquired thereafter it can be concluded that the porphyrin remaining adsorbed at the MgO nanocube surface is MgTPP (Figure 3). The determination of the porphyrin concentration in the washing solution yields the number of

DOI: 10.1021/acsami.5b08123
ACS Appl. Mater. Interfaces 2015, 7, 22962−22969

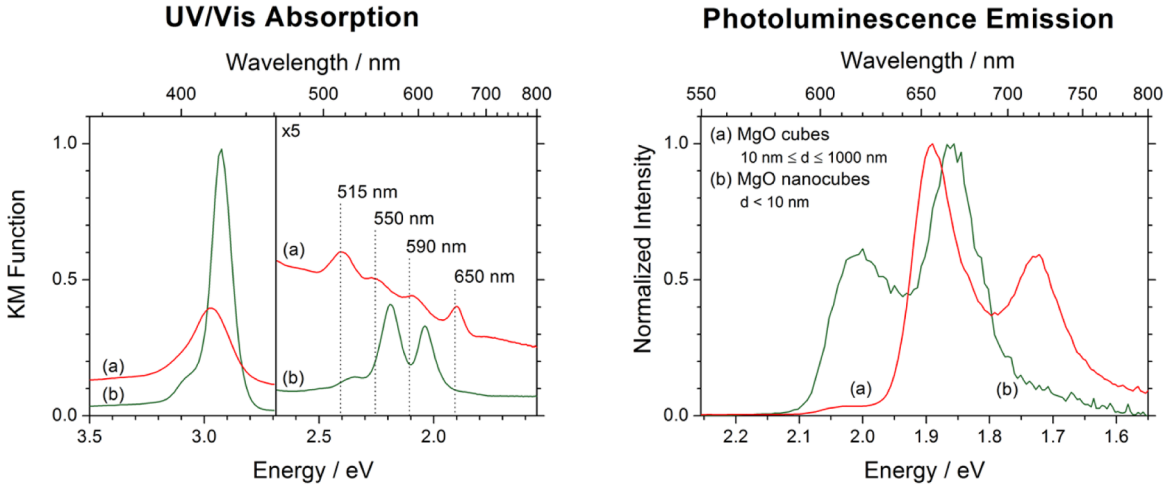

Figure 5. UV/vis DR (left) and photoluminescence spectra (right) of MgO cubes after 2HTPP adsorption (a) and MgO nanocubes after 2HTPP adsorption (b). In this experiment the initial 2HTPP concentrations in toluene correspond for nanocubes and cubes to 10^{-5} and 3×10^{-3} mol L^{-1}, respectively.

adsorbed molecules per MgO nanocube (Figure 4). For adsorption experiments with concentrations corresponding to the saturation region (i.e., $c \geq 3 \times 10^{-3}$ mol L^{-1}) the UV/vis spectra related to the solutions of the first two washing steps (for adsorption and washing procedure see Experimental Section) show absorption bands specific to 2HTPP. The intensity of the 2HTPP bands decreases continuously for washing solutions 3, 4, and 5, and only negligible contributions of MgTPP were observed.[25]

From this we conclude that MgTPP remains strongly adsorbed at the nanocube surface at room temperature, whereas 2HTPP is washed off almost quantitatively. It is important to note that exposure of MgO nanocube powder to porphyrin solutions of any concentration does not induce structural or morphological changes on the nanocrystals as concluded from a detailed TEM analysis from different parts of the powder sample (Figure S1; Figure 2). Powder X-ray diffraction measurements (Supporting Information, Figure S1) reveal that MgO periclase remains the exclusive crystalline phase after particle functionalization with porphyrins.

Significantly different observations are made for the optical properties of MgO powders, which consist of larger MgO smoke *cubes* (10 nm $\leq d \leq$ 1000 nm),[17] after steps i, dispersion in 2HTPP solutions; ii, washing with toluene; and iii, drying of the powder in high vacuum (Figure 5a), performed. The respective UV/vis DR spectrum shows a slightly broadened Soret-band at 2.95 eV (420 nm) (Figure 5a, left). In addition, four well-separated bands at 2.41 eV (515 nm), 2.28 eV (545 nm), 2.10 eV (590 nm), and 1.91 eV (650 nm) are observed. Comparison with the spectral region of the reference spectra for 2HTPP and MgTPP in solution (Figure 3, left) clearly reveals that the free-base porphyrin remains the prevailing adsorbate on the large MgO cubes. Further evidence for the preferential presence of 2HTPP is provided by PL spectroscopy: the emission spectrum exhibits two intense bands at 1.89 eV (655 nm) and 1.72 eV (720 nm) (Figure 5a, right), which are consistent with the PL emission fingerprint of 2HTPP in solution (Figure 3b). Moreover, the extremely high sensitivity of PL spectroscopy enables us to identify even minor contributions of the metalated porphyrin, that is, via the low intensity observed for the emission band at 2.00 eV (620 nm). The absence of the related feature in the DR spectrum (Figure 5a, left) is attributed to the significantly lower sensitivity of the latter technique.

The third independent spectroscopic evidence for porphyrin metalation is provided by DRIFTS (Figure 6) measurements.

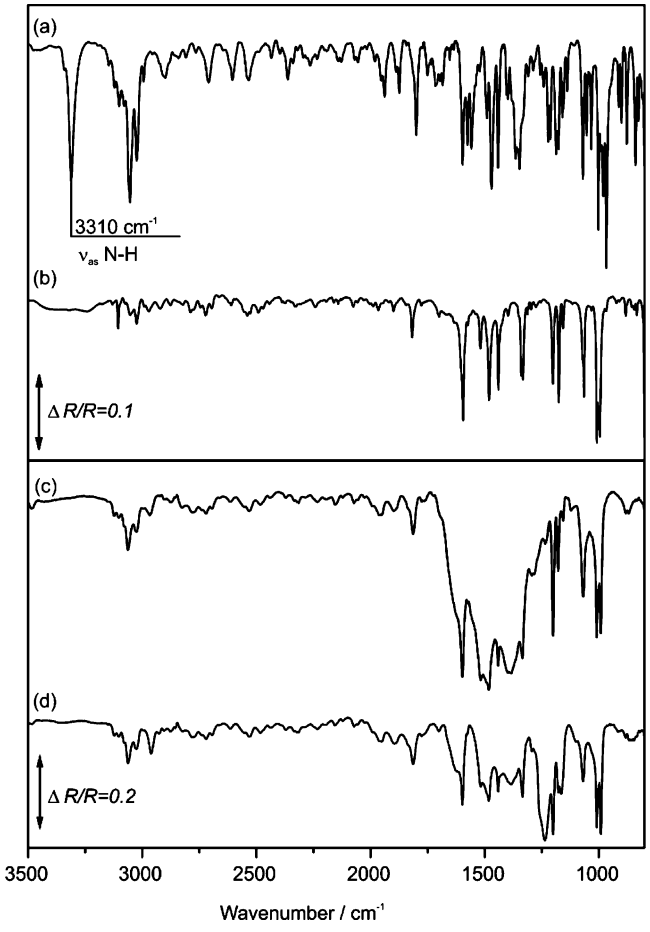

Figure 6. DRIFT spectra of pure and adsorbed 2HTPP and MgTPP: (top panel) reference spectra obtained on 2HTPP (a) and MgTPP (b) diluted in a KBr powder; (bottom panel) spectra obtained on MgO nanocubes after adsorption of 2HTPP (c) and MgTPP (d).

DOI: 10.1021/acsami.5b08123
ACS Appl. Mater. Interfaces 2015, 7, 22962−22969

MgO has strong absorptions in the MIR region below 1700 cm^{-1},[26] that is, in the fingerprint region of 2HTPP.[27,28] Preparatory experiments are described in the Supporting Information, which shows that relevant information can be obtained from this spectral region despite the low sample reflectivity (Figure S3).

The top spectra in Figure 6 were obtained on 2HTPP (a) and MgTPP (b), which was diluted in KBr and serves as a reference for the adsorption experiment. The sharp band at 3310 cm^{-1} (arrow in Figure 6a) corresponds to an asymmetric ν_{as}(N−H) stretching vibration, and its absence serves as an indicator for the metalation reaction. The features at 3170−2970 cm^{-1} are attributed to ν(C−H) vibrations. The features above ca. 3030 cm^{-1} are due to ν(C−H) vibrations in the porphyrin, and the features in the energy range below originate from IR active contributions of the phenyl rings. The less intense features between 2970 and 1610 cm^{-1} are attributed to overtones and combination vibrations.

The absence of ν_{as}(N−H) in the spectrum that was acquired on MgTPP (Figure 6b) characterizes the porphyrin in its metalated form. Features in the range between 3170 and 2970 cm^{-1} and in the region of overtone and combination bands display lower intensities in comparison to 2HTPP. Finally, the fingerprint region features less but well-separated absorptions.[27,28]

Figure 6c describes the situation after contacting 2HTPP with MgO nanocubes. This vibrational spectrum is consistent with that of MgTPP (Figure 6b,d). As outlined in the Supporting Information, variations in the relative intensity of the bands in comparison to the pure porphyrins in KBr are due to the low signal-to-noise ratio that results from the limited reflectivity of MgO in this spectral region. Contacting 2HTPP with larger MgO cubes (10 nm $\leq d \leq$ 1000 nm, not shown) did not reveal any significant absorptions above 1610 cm^{-1}. From the absence of any porphyrin-relevant IR signals from these cubes, we conclude that the concentration of adsorbed porphyrins is too low to allow for identification of porphyrin by DRIFTS in the case of this material.

DISCUSSION

The comparison of the adsorption behavior between MgO nanocubes with a particle size below 10 nm and larger MgO cubes with a size in the range of 10 nm $\leq d \leq$ 1000 nm reveals pronounced size effects in the porphyrin metalation reaction at the solid−liquid interface. The process of porphyrin adsorption and metalation levels off and finally saturates for MgO nanocubes at a coverage that corresponds to one monolayer of porphyrin molecules adsorbed in a flat-lying geometry. The vast majority of porphyrin adsorbs on MgO nanocubes in the metalated form. For larger MgO cubes, on the contrary, adsorbed porphyrins exist mainly as the free base. Apparently, only a small fraction of the surface sites is capable of donating Mg^{2+} ions and deprotonating the porphyrin. In accordance with recent DFT calculations[29] we attribute this structure dependence to the presence of low coordinated Mg sites, for example, corners and edges:

$$2\text{HTPP} + (\text{MgO})_n \rightarrow \text{MgTPP} + \text{Mg}_{n-1}\text{O}_{n-2}(\text{OH})_2 \quad (1)$$

The two protons, which are released by the free-base porphyrin after the uptake of the Mg^{2+} ion, are expected to convert two surface oxygen anions into OH groups.[29] We assume that the limited mobility of MgTPP at the surface of MgO nanocubes and cubes confines the molecules to the close proximity of those reactive corner or edge sites where porphyrin metalation takes place. Consequently, the process of porphyrin metalation and adsorption would be self-limiting provided that neither MgTPP diffusion to the center of the (100) terraces nor porphyrin desorption into the toluene bulk contributes to the recovery of the reactive sites. Indeed, we observe that the porphyrins, once metalated at the MgO surface, remain adsorbed even after repeated washing cycles with the pure solvent. More importantly, no significant morphological changes, which could give rise to the formation of new reactive sites, are observed. Considering a nanocube with an edge length of 4.5 nm and assuming an area of 2 nm^2 as the spatial requirement of the flat porphyrin molecule, around 80% of the whole surface would be covered if MgTPP adsorption was limited to the close proximity of the nanocube corners and edges, as schematically illustrated in Figure 7. On the contrary, only ∼1% of the surface would be covered in the case of a cube with an edge length of 450 nm. Consequently, a significantly higher surface fraction is available for the physisorption of the free base on larger cubes, which seems to take place at extended (100) terraces. This is consistent with our observation that on the large MgO cubes only a minor fraction of the adsorbed porphyrin is metalated, whereas the majority exists as the free base. Importantly, the same molecular interactions are expected between 2HTPP and low-coordinated surface sites on MgO cubes and nanocubes. The adsorption properties of the respective particle powder, however, critically depend on the relative abundance of corner and edge sites, which are able to trigger porphyrin metalation, and of terrace sites, where porphyrin physisorption is expected to take place.[29] From another perspective, the concentration limit observed for adsorptive porphyrin metalation (Figure 4) implies the absence of multilayer adsorption. Interestingly, this result carries the potential for the preparation of metal oxide hybrid structures with controlled coverages of adsorbed functional molecules.

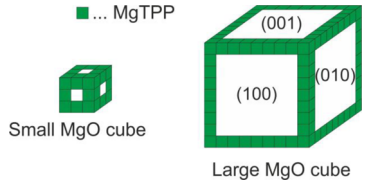

Figure 7. Scheme illustrating proposed MgTPP adsorption at sites in close proximity of corner and edge sites of the MgO cubes, where porphyrin metalation and oxide hydroxylation are expected to occur. On large cubes only a limited surface fraction would be covered by MgTPP, the major part of the surface being available for the adsorption of the free base.

MgO particles represent a class of thermally exceptionally stable nanomaterials with a high level of morphological definition. Nanocubes (Figure 2) exhibit a high proportion of surface edge and corner features with specific electronic characteristics and reactivity.[7,18,30] Further control over the chemistry at organic−inorganic interfaces in combination with advances in the site specificity and spatial organization of the adsorbed porphyrins will enhance our abilities to organize particles and porphyrins at a supramolecular level.[31] In this respect the metalation reaction in combination with the saturation limit observed for adsorption (Figure 4) may lead to a promising new method to adjust the interaction between

DOI: 10.1021/acsami.5b08123
ACS Appl. Mater. Interfaces 2015, 7, 22962−22969

metal oxide nanoparticles and photoactive molecules. This method takes advantage of interaction forces that are beyond those commonly used, that is, covalent bonding, hydrogen bonding, van der Waals interaction, and $\pi-\pi$ interactions.[31]

CONCLUSIONS

Here we report very first evidence of ion exchange reactions between oxide nanostructures and free base porphyrins at the solid−liquid interface. The adsorption of 2HTPP on MgO particle powders is governed by the relative abundance of low-coordinated surface sites. Our results point to porphyrin metalation at corner and edge sites of MgO nanocubes and larger MgO cubes and provide unambiguous evidence for MgTPP adsorption at coordinatively unsaturated sites of the MgO cube surfaces. Terrace sites, on the other hand, seem to bind porphyrin molecules more weakly by physisorption. The potential site specificity of porphyrin metalation and adsorption constitutes a promising approach for the spatial organization of photoactive molecules in metal oxide hybrid structures. Last but not least, our study emphasizes the importance of an integrated characterization approach. Complementary spectroscopies are the key to following the self-organization of the porphyrin−metal oxide supramolecular arrangements.

ASSOCIATED CONTENT

Supporting Information

The Supporting Information is available free of charge on the ACS Publications website at DOI: 10.1021/acsami.5b08123.

X-ray diffractograms and additional transmission electron micrographs of MgO nanocube powders before and after porphyrin adsorption as well as results of preparatory DRIFTS experiments and further experimental details (PDF)

AUTHOR INFORMATION

Corresponding Authors

*(J.L.) E-mail: joerg.libuda@fau.de.

*(T.B.) E-mail: thomas.berger@sbg.ac.at.

Notes

The authors declare no competing financial interest.

ACKNOWLEDGMENTS

This project was financially supported by the Deutsche Forschungsgemeinschaft (DFG) within the Research Unit FOR 1878 "funCOS − Functional Molecular Structures on Complex Oxide Surfaces". We acknowledge additional support from the Excellence Cluster "Engineering of Advanced Materials" within the framework of the excellence initiative. We also acknowledge support by COST Action CM1104 "Reducible oxide chemistry, structure and functions".

REFERENCES

(1) Gómez-Romero, P.; Sanchez, C. *Functional Hybrid Materials*; Wiley-VCH: Weinheim, Germany, 2004.

(2) Kickelbick, G. *Hybrid Materials: Synthesis, Characterization, and Applications*; Wiley-VCH: Weinheim, Germany, 2007.

(3) Berger, T.; Diwald, O. Defects in Metal Oxide Nanoparticle Powders. In *Defects at Oxide Surfaces*; Jupille, J., Thornton, G., Eds.; Springer International Publishing: Cham, Switzerland, 2015.

(4) Wang, W.; Xie, N.; He, L.; Yin, Y. Photocatalytic Colour Switching of Redox Dyes for Ink-free Light-printable Rewritable Paper. *Nat. Commun.* **2014**, *5*, 5459.

(5) Mills, A.; Wells, N. Reductive Photocatalysis and Smart Inks. *Chem. Soc. Rev.* **2015**, *44*, 2849.

(6) Kim, B.; Park, S. W.; Kim, J.-Y.; Yoo, K.; Lee, J. A.; Lee, M.-W.; Lee, D.-K.; Kim, J. Y.; Kim, B.; Kim, H.; Han, S.; Son, H. J.; Ko, M. J. Rapid Dye Adsorption via Surface Modification of TiO_2 Photoanodes for Dye-sensitized Solar Cells. *ACS Appl. Mater. Interfaces* **2013**, *5*, 5201−5207.

(7) Sternig, A.; Diwald, O.; Gross, S.; Sushko, P. V. Surface Decoration of MgO Nanocubes with Sulfur Oxides: Experiment and Theory. *J. Phys. Chem. C* **2013**, *117*, 7727−7735.

(8) Baer, D. R.; Engelhard, M. H.; Johnson, G. E.; Laskin, J.; Lai, J.; Mueller, K.; Munusamy, P.; Thevuthasan, S.; Wang, H.; Washton, N.; Elder, A.; Baisch, B. L.; Karakoti, A.; Kuchibhatla, S. V. N. T.; Moon, D. Surface Characterization of Nanomaterials and Nanoparticles: Important Needs and Challenging Opportunities. *J. Vac. Sci. Technol., A* **2013**, *31*, 50820.

(9) Taguchi, T.; Zhang, X.-T.; Sutanto, I.; Tokuhiro, K.-I.; Rao, T. N.; Watanabe, H.; Nakamori, T.; Uragam, M.; Fujishima, A. Improving the Performance of Solid-state Dye-sensitized Solar Cell using MgO-coated TiO_2 Nanoporous Film. *Chem. Commun.* **2003**, *9*, 2480−2481.

(10) Kay, A.; Grätzel, M. Dye-sensitized Core-shell Nanocrystals: Improved Efficiency of Mesoporous Tin Oxide Electrodes Coated with a Thin Layer of an Insulating Oxide. *Chem. Mater.* **2002**, *14*, 2930−2935.

(11) Docampo, P.; Tiwana, P.; Sakai, N.; Miura, H.; Herz, L.; Murakami, T.; Snaith, H. J. Unraveling the Function of an MgO Interlayer in both Electrolyte and Solid-state SnO_2 Based Dye-sensitized Solar Cells. *J. Phys. Chem. C* **2012**, *116*, 22840−22846.

(12) Tian, P.; Han, X.-Y.; Ning, G.-L.; Fang, H.-X.; Ye, J.-W.; Gong, W.-T.; Lin, Y. Synthesis of Porous Hierarchical MgO and its Superb Adsorption Properties. *ACS Appl. Mater. Interfaces* **2013**, *5*, 12411−12418.

(13) Ai, L.; Yue, H.; Jiang, J. Sacrificial Template-directed Synthesis of Mesoporous Magnesium Oxide Architectures with Superior Performance for Organic Dye Adsorption. *Nanoscale* **2012**, *4*, 5401−5408.

(14) Knözinger, E.; Diwald, O.; Sterrer, M. Chemical Vapour Deposition − A New Approach to Reactive Surface Defects of Uniform Geometry on High Surface Area Magnesium Oxide. *J. Mol. Catal. A: Chem.* **2000**, *162*, 83−95.

(15) Siedl, N.; Gügel, P.; Diwald, O. Synthesis and Aggregation of In_2O_3 Nanoparticles: Impact of Process Parameters on Stoichiometry Changes and Optical Properties. *Langmuir* **2013**, *29*, 6077−6083.

(16) Siedl, N.; Koller, D.; Sternig, A. K.; Thomele, D.; Diwald, O. Photoluminescence Quenching in Compressed MgO Nanoparticle Systems. *Phys. Chem. Chem. Phys.* **2014**, *16*, 8339−8345.

(17) Baumann, S. O.; Schneider, J.; Sternig, A.; Thomele, D.; Stankic, S.; Berger, T.; Grönbeck, H.; Diwald, O. Size Effects in MgO Cube Dissolution. *Langmuir* **2015**, *31*, 2770−2776.

(18) McKenna, K. P.; Koller, D.; Sternig, A.; Siedl, N.; Govind, N.; Sushko, P. V.; Diwald, O. Optical Properties of Nanocrystal Interfaces in Compressed MgO Nanopowders. *ACS Nano* **2011**, *5*, 3003−3009.

(19) Diwald, O.; Sterrer, M.; Knözinger, E. Site Selective Hydroxylation of the MgO Surface. *Phys. Chem. Chem. Phys.* **2002**, *4*, 2811−2817.

(20) Edwards, L.; Dolphin, D.; Gouterman, M.; Adler, A. Porphyrins XVII. Vapor Absorption Spectra and Redox Reactions: Tetraphenylporphins and Porphin. *J. Mol. Spectrosc.* **1971**, *38*, 16−32.

(21) Gouterman, M. Study of the Effects of Substitution on the Absorption Spectra of Porphin. *J. Chem. Phys.* **1959**, *30*, 1139.

(22) Rubio, M.; Roos, B. O.; Serrano-Andrés, L.; Merchán, M. Theoretical Study of the Electronic Spectrum of Magnesium-porphyrin. *J. Chem. Phys.* **1999**, *110*, 7202.

(23) Röckert, M.; Franke, M.; Tariq, Q.; Lungerich, D.; Jux, N.; Stark, M.; Kaftan, A.; Ditze, S.; Marbach, H.; Laurin, M.; Libuda, J.; Steinrück, H.-P.; Lytken, O. Insights in Reaction Mechanistics: Isotopic Exchange During the Metalation of Deuterated Tetraphenyl-21,23 D-Porphyrin on Cu(111). *J. Phys. Chem. C* **2014**, *118*, 26729−26736.

DOI: 10.1021/acsami.5b08123
ACS Appl. Mater. Interfaces 2015, 7, 22962−22969

(24) Shubina, T. E.; Marbach, H.; Flechtner, K.; Kretschmann, A.; Jux, N.; Buchner, F.; Steinrück, H.-P.; Clark, T.; Gottfried, J. M. Principle and Mechanism of Direct Porphyrin Metalation: Joint Experimental and Theoretical Investigation. *J. Am. Chem. Soc.* **2007**, *129*, 9476−9483.
(25) This contribution may either result (i) from traces of MgO particles (with adsorbed MgTPP) remaining in suspension after centrifugation or (ii) from the desorption of MgTPP from the nanocube surface upon washing with the pure solvent. Considering case ii, the amount of MgTPP desorbed in the course of washing steps 3−5 corresponds to only ∼0.6% of a monolayer.
(26) Kumar, A.; Kumar, J. On the Synthesis and Optical Absorption Studies of Nano-size Magnesium Oxide Powder. *J. Phys. Chem. Solids* **2008**, *69*, 2764−2772.
(27) Zhang, X.; Zhang, Y.; Jiang, J. Infrared Spectra of Metal-free, N′,N-dideuterio, and Magnesium Porphyrins: Density Functional Calculations. *Spectrochim. Acta, Part A* **2005**, *61*, 2576−2583.
(28) Zhang, J.; Zhang, P.; Zhang, Z.; Wei, X. Spectroscopic and Kinetic Studies of Photochemical Reaction of Magnesium Tetraphenylporphyrin with Oxygen. *J. Phys. Chem. A* **2009**, *113*, 5367−5374.
(29) Schneider, J.; Franke, M.; Gurrath, M.; Röckert, M.; Berger, T.; Bernardi, J.; Meyer, B.; Steinrück, H.-P.; Lytken, O.; Diwald, O. Porphyrin Metalation at MgO Surfaces: a Spectroscopic and Quantum Mechanical Study on Complementary Model Systems. *Chem. Eur. J.*, **2015**, submitted for publication.
(30) Cadigan, C. A.; Corpuz, A. R.; Lin, F.; Caskey, C. M.; Finch, K. B. H.; Wang, X.; Richards, R. M. Nanoscale (111) Faceted Rock-salt Metal Oxides in Catalysis. *Catal. Sci. Technol.* **2013**, *3*, 900−911.
(31) Hasobe, T. Porphyrin-based Supramolecular Nanoarchitectures for Solar Energy Conversion. *J. Phys. Chem. Lett.* **2013**, *4*, 1771−1780.

DOI: 10.1021/acsami.5b08123
ACS Appl. Mater. Interfaces 2015, 7, 22962−22969